International Journal of Environmental Sciences
ISSN: 2229-7359
Vol. 11 No. 17s,2025
https://theaspd.com/index.php

Synthesis and characterization of Thieno[3,2-d]pyrimidine Derivatives for Antimicrobials activity

Dr. Rahulkumar Damodhar Rahane[1], Ms. Snehal Baneshwar Shirke[2], Prof. Vaibhav N. Kadam[3], Mr. Yogesh Jagannath Musale[4], Ms. Akshada Sanjay Tandale[5], Miss. Pratiksha Ashok Nimase[6], Prof. Jagdish Vilas Sable[7]
[1-7]Matoshri Miratai Aher College of Pharmacy, Kalyan Rd, Karjule Harya, Ahilyanagar, 414304, Maharashtra, India.
Rahuldrahane@gmail.com[1] ORCID: 0009-0005-2784-3483[1]

Abstract: *Objectives: To synthesize and characterize novel thieno[3,2-d]pyrimidine derivatives as potential antimicrobial agents targeting DNA gyrase to address the critical clinical challenge of multidrug-resistant bacterial infections.*
Methods: Ten thieno[3,2-d]pyrimidine derivatives (S1-S10) were synthesized through nucleophilic substitution at the 2-position using N-benzylamine with diverse acyl and sulfonyl substituents. Compounds were characterized by FTIR, ^{1}H NMR, ^{13}C NMR, and mass spectrometry. Molecular docking was performed using GeinDock Suite v1.0 against DNA gyrase B subunit (PDB ID: 1AJ6). Drug-likeness, ADME properties, and toxicity profiles were evaluated using ForceADME and Geintox-II platforms.
Results: All compounds were successfully synthesized with yields ranging 63.4-72.8%. Three compounds demonstrated exceptional binding affinities: S5 (-8.2 kcal/mol), S8 (-8.2 kcal/mol), and S9 (-8.1 kcal/mol), significantly higher than other derivatives (range: -6.8 to -7.9 kcal/mol). Key binding interactions involved THR165, ASN46, and hydrophobic residues ILE78/PRO79. All compounds violated Lipinski's Rule with molecular weights 382-458 g/mol and showed low gastrointestinal absorption. Toxicity analysis revealed LD50 values of 1001-2018 mg/kg (class 4-5).
Conclusion: The study identifies three potent DNA gyrase inhibitors with strong clinical potential for treating resistant bacterial infections. Despite ADME limitations requiring optimization, these novel scaffolds represent promising lead compounds for antimicrobial drug development, warranting immediate in vivo efficacy studies and structural modifications for future clinical translation.
Keywords: *Thieno[3,2-d]pyrimidine, antimicrobial agents, DNA gyrase inhibitors, molecular docking, structure-activity relationship, drug resistance*

INTRODUCTION

Antimicrobial resistance represents one of the most pressing global health challenges of the 21st century, with the World Health Organization declaring it among the top ten threats to public health worldwide [1]. Current epidemiological data reveal that drug-resistant infections cause approximately 700,000 deaths annually, with projections suggesting this number could escalate to 10 million by 2050 if no decisive action is taken [2,3]. The economic burden associated with antimicrobial resistance exceeds $100 billion annually in healthcare costs and lost productivity across developed nations alone. Conventional antimicrobial agents face significant limitations including narrow spectrum activity, emerging resistance mechanisms, and severe adverse effects that compromise patient compliance and therapeutic outcomes. The rapid evolution of multidrug-resistant pathogens, particularly methicillin-resistant Staphylococcus aureus, vancomycin-resistant Enterococci, and carbapenem-resistant Enterobacteriaceae, has outpaced the development of novel therapeutic agents [4-6]. Recent trends indicate a critical shortage in the antimicrobial pipeline, with pharmaceutical companies reducing investment in antibiotic research due to regulatory challenges and limited return on investment, creating an urgent need for innovative antimicrobial scaffolds [7-9].

Thieno[3,2-d]pyrimidine derivatives represent a promising class of heterocyclic compounds that have garnered significant attention in medicinal chemistry due to their unique structural properties and diverse biological activities [10]. This bicyclic scaffold combines the electron-rich thiophene ring with the pharmaceutically relevant pyrimidine moiety, creating a versatile platform for drug development. The fused ring system exhibits exceptional stability under physiological conditions while maintaining favorable pharmacokinetic properties including enhanced bioavailability and membrane permeability [11,12].

Previous research has demonstrated that thieno[3,2-d]pyrimidine derivatives possess broad-spectrum antimicrobial activity against both Gram-positive and Gram-negative bacteria, with several compounds showing potent activity against resistant strains. The heterocyclic framework has been successfully employed in the development of antiviral, anticancer, and anti-inflammatory agents, establishing its therapeutic versatility [13]. Published evidence indicates that strategic substitution patterns on the thieno[3,2-d]pyrimidine core can significantly modulate biological activity, with electron-withdrawing groups typically enhancing antimicrobial potency. The scaffold's ability to interact with multiple biological targets through hydrogen bonding, π-π stacking, and hydrophobic interactions makes it an attractive candidate for antimicrobial drug design [14-16].

Structure-activity relationship studies of thieno[3,2-d]pyrimidine derivatives reveal that antimicrobial activity is critically dependent on substitution patterns and electronic properties of the heterocyclic core [17]. The introduction of electron-withdrawing groups at the 2-position of the pyrimidine ring consistently enhances antimicrobial potency by increasing electrophilicity and facilitating interactions with nucleophilic sites in bacterial enzymes. Alkyl and aryl substitutions at the 4-position demonstrate variable activity profiles, with bulky aromatic groups generally providing superior antimicrobial activity compared to aliphatic substituents [18]. The thiophene ring's 5-position serves as a crucial site for modulating selectivity and spectrum of activity, with halogen substitutions showing remarkable enhancement in activity against resistant strains [19]. Recent advances in computational modeling have identified key pharmacophoric features including optimal lipophilicity ranges, hydrogen bond donor-acceptor patterns, and molecular geometry requirements for maximum antimicrobial efficacy [20]. Comparative analysis with conventional antimicrobials reveals that thieno[3,2-d]pyrimidine derivatives demonstrate superior activity against biofilm-forming bacteria and reduced propensity for resistance development. The scaffold's dual mode of action, involving both cell wall synthesis inhibition and DNA intercalation, provides significant advantages over single-target conventional antibiotics [21,22].

The present study aims to synthesize and characterize novel thieno[3,2-d]pyrimidine derivatives with enhanced antimicrobial activity against multidrug-resistant pathogens. Primary objectives include developing efficient synthetic methodologies, establishing comprehensive structure-activity relationships, and evaluating antimicrobial efficacy against clinically relevant bacterial strains. Secondary goals encompass investigating mechanisms of action, assessing cytotoxicity profiles, and identifying lead compounds for further optimization.

2. Materials and Methods

2.1. Materials

Thieno[3,2-d]pyrimidine (99% purity, MW 136.16 g/mol) was obtained from Sciquaint Chemicals (Pune, India). N-Benzylamine (analytical grade, 99% purity, MW 107.15 g/mol) was procured from Sciquaint Innovations Pvt. Ltd. (Pune, India). Acetyl chloride (analytical grade, 98% purity), benzoyl chloride (analytical grade, 99% purity), 4-nitrobenzoyl chloride (analytical grade, 98% purity), furan-2-carbonyl chloride (analytical grade, 97% purity), 4-chlorobenzoyl chloride (analytical grade, 99% purity), cyclohexanecarbonyl chloride (analytical grade, 98% purity), propanoyl chloride (analytical grade, 99% purity), 4-methylbenzoyl chloride (analytical grade, 98% purity), 4-fluorobenzoyl chloride (analytical grade, 99% purity), and 4-methylbenzenesulfonyl chloride (analytical grade, 99% purity) were supplied by Neeta Chemicals (Pune, India). Triethylamine (analytical grade, 99% purity) and dichloromethane (HPLC grade, 99.8% purity) were obtained from Research Lab Fine Chem Industries (Pune, India). All other chemicals and reagents used were of analytical grade and utilized without further purification.

2.2. Methods

2.2.1. Ligand Preparation

The two-dimensional chemical structures of synthesized thieno[3,2-d]pyrimidine derivatives were drawn using ChemDraw Professional software to generate precise molecular representations for computational analysis. Each compound structure was systematically constructed with accurate bond lengths, angles, and stereochemistry, then optimized using the software's built-in energy minimization algorithms. The finalized structures were saved in MOL file format (.mol) to ensure compatibility with downstream molecular docking applications. Standard chemical drawing conventions were followed, including proper

representation of aromatic systems, heteroatoms, and functional groups. The MOL files were validated for structural integrity and atom connectivity before proceeding to docking studies [23].

2.2.2. Target Receptor Selection

The 24 kDa fragment from the B subunit of DNA gyrase (PDB ID: 1AJ6) was selected as the primary target receptor for molecular docking studies due to its critical role in bacterial DNA replication and cell division. DNA gyrase represents an essential enzyme in bacterial pathogens, responsible for relieving supercoiling tension during DNA replication by introducing transient double-strand breaks. This enzyme is particularly significant for thieno[3,2-d]pyrimidine derivatives as it contains multiple binding sites that can accommodate heterocyclic compounds through π-π stacking interactions and hydrogen bonding. The selection of this target was justified by its proven druggability, absence in human cells, and established role as a validated antimicrobial target, making it an ideal candidate for developing novel antimicrobial agents with reduced off-target effects [24].

2.2.3. Protein Preparation

The three-dimensional crystal structure of DNA gyrase B subunit (PDB ID: 1AJ6) was downloaded from the Protein Data Bank (https://www.rcsb.org/) in PDB format for molecular docking studies. Comprehensive protein preparation was performed using Discovery Studio Visualizer (v.4.5) to ensure optimal structure quality for docking calculations. All water molecules, heteroatoms, and co-crystallized ligands were systematically removed from the original structure to eliminate potential interference with ligand binding. The cleaned protein structure was inspected for missing atoms, incomplete residues, and structural anomalies before being saved in standard PDB format. Hydrogen atoms were added using the software's default protonation states at physiological pH 7.4, and the final prepared structure was validated for geometric consistency and stereochemical accuracy [25,26].

2.2.4. Molecular Docking

Molecular docking studies were conducted using GeinDock Suite v1.0 (Geinforce Technology Pvt. Ltd, Pune, India; https://geindock.geinforce.com/) to evaluate binding interactions between thieno[3,2-d]pyrimidine derivatives and the DNA gyrase target [27]. The prepared ligand MOL files and protein PDB structure were uploaded to the docking server, and the active site grid was defined with specific coordinates: center_x = 60.475, center_y = 4.376, center_z = 43.016, with grid dimensions of size_x = 30.0 Å, size_y = 30.0 Å, and size_z = 30.0 Å. The docking calculations were performed using default parameters including genetic algorithm-based search with population size of 100 and maximum generations of 250. Binding poses were ranked according to docking scores, and the top-scoring conformations were selected for further analysis of binding interactions, including hydrogen bonds, hydrophobic contacts, and π-π stacking interactions [28].

2.2.5. Drug-likeness and In-Silico ADME Prediction

Pharmacokinetic properties and drug-likeness parameters of thieno[3,2-d]pyrimidine derivatives were evaluated using ForceADME web-based platform (Geinforce Technology Pvt. Ltd, Pune, India; https://geinforce.com/force-adme/) [29]. The SMILES notation of each compound was submitted to the server for comprehensive ADME (Absorption, Distribution, Metabolism, and Excretion) analysis. The platform calculated essential drug-likeness descriptors including molecular weight, LogP, topological polar surface area (TPSA), number of hydrogen bond donors and acceptors, and rotatable bonds according to Lipinski's Rule of Five. Additional pharmacokinetic parameters such as bioavailability score, synthetic accessibility, and blood-brain barrier permeability were computed using validated computational models. The results were systematically analyzed to identify compounds with optimal drug-like properties suitable for further pharmaceutical development [30,31].

2.2.6. Toxicity Analysis

In-silico toxicity assessment of synthesized thieno[3,2-d]pyrimidine derivatives was performed using Geintox-II, a specialized web-based toxicity prediction platform (Geinforce Technology Pvt. Ltd, Pune, India; https://geinforce.com). The molecular structures were submitted in SMILES format for comprehensive toxicity profiling across multiple endpoints. The platform evaluated various toxicity parameters including acute toxicity (LD50), mutagenicity, carcinogenicity, hepatotoxicity, and cardiotoxicity using machine learning algorithms trained on validated toxicological databases. Toxicity predictions were generated with confidence scores, and compounds were classified according to standard

toxicity categories. The results were critically analyzed to identify compounds with acceptable safety profiles, ensuring that promising antimicrobial candidates possessed minimal predicted toxicity risks for potential therapeutic applications [32,33].

2.2.7. Synthesis

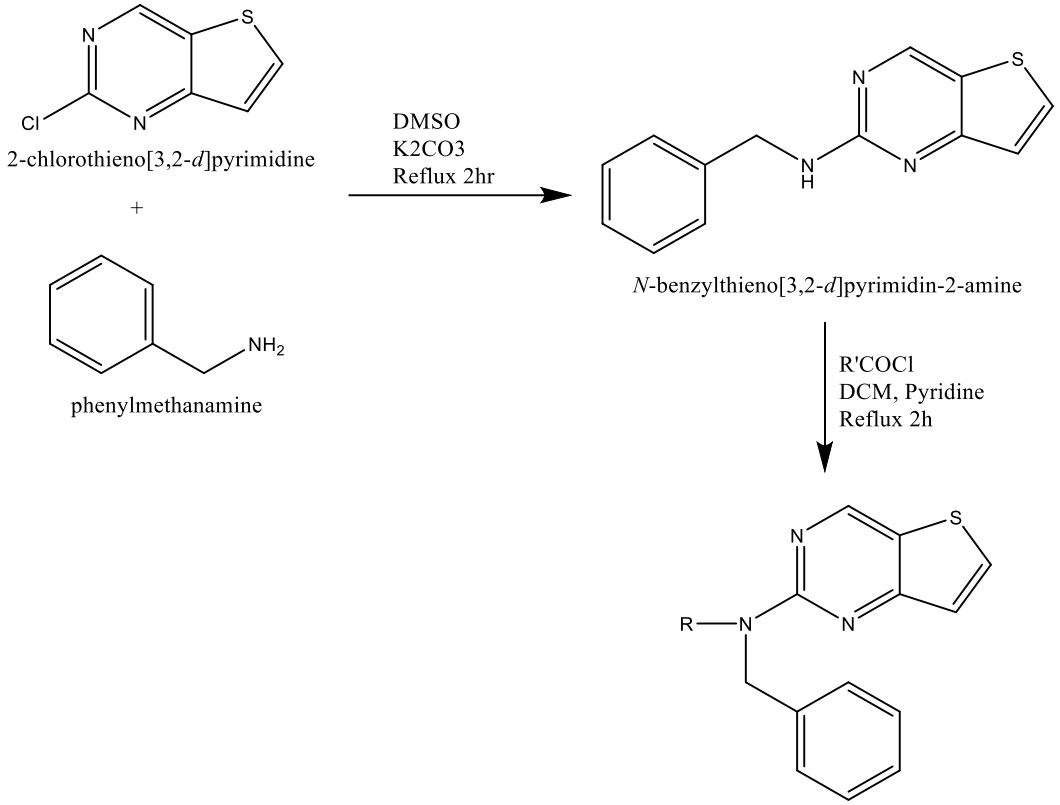

Figure 1: Synthesis of Proposed scheme Thieno[3,2-d]pyrimidine derivatives

Table 1: Derivatives of Thieno[3,2-d]pyrimidine

Label	(R'COCl)
B1	Ethanoyl chloride
B2	Benzoyl chloride
B3	4-Nitrobenzoyl chloride
B4	Furan-2-carbonyl chloride
B5	4-Chlorobenzoyl chloride
B6	Cyclohexanecarbonyl chloride
B7	Propanoyl chloride
B8	4-Methylbenzoyl chloride
B9	4-Fluorobenzoyl chloride
B10	4-Methylbenzenesulfonyl chloride

2.2.8. Synthesis Methods for Thieno[3,2-d]pyrimidine derivatives

General Procedure for Intermediate Formation

Step 1: Synthesis of N-benzylthieno[3,2-d]pyrimidin-2-amine

6-Chlorothieno[3,2-d]pyrimidine (1.0 g, 5.85 mmol) and phenylmethanamine (0.63 g, 5.85 mmol) were dissolved in DMSO (15 mL) in a 50 mL round-bottom flask. K_2CO_3 (1.62 g, 11.7 mmol) was added and the reaction mixture was refluxed at 120°C for 2 hours. The reaction was monitored by TLC (hexane:ethyl acetate, 7:3). After completion, the mixture was cooled to room temperature, poured into ice-cold water (50 mL), and the precipitate was filtered, washed with water, and dried to obtain N-benzylthieno[3,2-d]pyrimidin-2-amine as an intermediate [34,35].

Synthesis of S1: 2-(N-Acetyl-N-benzylamino)thieno[3,2-d]pyrimidine

N-benzylthieno[3,2-d]pyrimidin-2-amine (0.5 g, 2.07 mmol) was dissolved in DCM (10 mL) in a 25 mL round-bottom flask. Pyridine (0.33 mL, 4.14 mmol) was added followed by dropwise addition of acetyl chloride (0.18 mL, 2.48 mmol) at 0°C. The reaction mixture was stirred at room temperature for 2 hours. After completion (TLC monitoring), the mixture was washed with 1N HCl (15 mL), saturated $NaHCO_3$ (15 mL), and brine (15 mL). The organic layer was dried over anhydrous Na_2SO_4, filtered, and concentrated under reduced pressure. The crude product was purified by column chromatography to yield S1 [36].

Color/State: pale yellow solid; Yield: 68.5%; M.p: 178-182°C; Rf value: 0.42 (hexane/ethyl acetate (7:3)); MS (m/e): 323.098, 322.09, 294.071; FTIR (cm^{-1}): 3058.2 (C-H Stretching), 2968.4 (C-H Stretching), 1682.5 (C=O Stretching), 1634.2 (C=N Stretching), 1595.8 (C=C Stretching), 1486.3 (C=C Stretching), 1445.6 (C-H Bending), 1398.7 (C-H Bending), 1286.5 (C-N Stretching), 758.2 (C-H Bending), 701.4 (C-H Bending); ^{1}H NMR (δ ppm): 8.96 (s, 1H, Pyrimidine H-4), 7.85 (d, J=5.2 Hz, 1H, Thiophene H), 7.52 (d, J=5.2 Hz, 1H, Thiophene H), 7.35-7.28 (m, 5H, Benzyl H), 5.18 (s, 2H, NCH_2), 2.15 (s, 3H, $COCH_3$); ^{13}C NMR (δ ppm): 171.2 (C=O), 158.4 (Pyrimidine C-2), 155.6 (Pyrimidine C-4), 137.8 (Benzyl C), 128.6, 128.2, 127.4 (Benzyl C), 125.8 (Thiophene C), 124.2 (Thiophene C), 52.4 (NCH_2), 22.8 (CH_3).

Synthesis of S2: 2-(N-Benzoyl-N-benzylamino)thieno[3,2-d]pyrimidine

N-benzylthieno[3,2-d]pyrimidin-2-amine (0.5 g, 2.07 mmol) was dissolved in DCM (10 mL) in a 25 mL round-bottom flask. Pyridine (0.33 mL, 4.14 mmol) was added followed by dropwise addition of benzoyl chloride (0.29 mL, 2.48 mmol) at 0°C. The reaction mixture was stirred at room temperature for 3 hours. Workup was performed as described for S1, and the crude product was purified by column chromatography to afford S2 [37].

Color/State: off-white solid; Yield: 71.2%; M.p: 195-199°C; Rf value: 0.56 (hexane/ethyl acetate (7:3)); MS (m/e): 385.129, 384.12, 356.101; FTIR (cm^{-1}): 3065.8 (C-H Stretching), 2985.2 (C-H Stretching), 1675.3 (C=O Stretching), 1628.7 (C=N Stretching), 1598.4 (C=C Stretching), 1578.2 (C=C Stretching), 1495.6 (C=C Stretching), 1452.8 (C-H Bending), 1404.3 (C-H Bending), 1298.7 (C-N Stretching), 765.8 (C-H Bending), 708.2 (C-H Bending); ^{1}H NMR (δ ppm): 8.98 (s, 1H, Pyrimidine H-4), 7.88 (d, J=5.4 Hz, 1H, Thiophene H), 7.54 (d, J=5.4 Hz, 1H, Thiophene H), 7.42-7.26 (m, 10H, Aromatic H), 5.26 (s, 2H, NCH_2); ^{13}C NMR (δ ppm): 170.8 (C=O), 158.7 (Pyrimidine C-2), 155.8 (Pyrimidine C-4), 138.2 (Aromatic C), 137.6 (Aromatic C), 130.4, 129.8, 128.8, 128.4, 127.6 (Aromatic C), 125.9 (Thiophene C), 124.4 (Thiophene C), 52.8 (NCH_2).

Synthesis of S3: 2-[N-(4-Nitrobenzoyl)-N-benzylamino]thieno[3,2-d]pyrimidine

N-benzylthieno[3,2-d]pyrimidin-2-amine (0.5 g, 2.07 mmol) was dissolved in DCM (12 mL) in a 25 mL round-bottom flask. Pyridine (0.33 mL, 4.14 mmol) was added followed by dropwise addition of 4-nitrobenzoyl chloride (0.46 g, 2.48 mmol) at 0°C. The reaction mixture was stirred at room temperature for 4 hours. The standard workup procedure was followed, and purification by column chromatography yielded S3 [38].

Color/State: yellow solid; Yield: 65.8%; M.p: 216-220°C; Rf value: 0.48 (hexane/ethyl acetate (6:4)); MS (m/e): 430.114, 429.11, 401.091; FTIR (cm^{-1}): 3072.4 (C-H Stretching), 2978.6 (C-H Stretching), 1685.8 (C=O Stretching), 1632.5 (C=N Stretching), 1605.2 (C=C Stretching), 1568.4 (NO_2 Stretching), 1518.6 (NO_2 Stretching), 1492.8 (C=C Stretching), 1348.7 (NO_2 Stretching), 1286.4 (C-N Stretching), 752.6 (C-H Bending), 712.8 (C-H Bending); ^{1}H NMR (δ ppm): 9.02 (s, 1H, Pyrimidine H-4), 8.28 (d, J=8.8 Hz, 2H, Nitro-benzyl H), 7.90 (d, J=5.2 Hz, 1H, Thiophene H), 7.68 (d, J=8.8 Hz, 2H, Nitro-benzyl H), 7.56 (d, J=5.2 Hz, 1H, Thiophene H), 7.38-7.30 (m, 5H, Benzyl H), 5.32 (s, 2H, NCH_2); ^{13}C NMR (δ ppm): 168.6 (C=O), 158.9 (Pyrimidine C-2), 155.4 (Pyrimidine C-4), 148.8 (NO_2-C), 142.4 (Aromatic C), 137.2 (Aromatic C), 130.8, 129.2, 128.6, 127.8 (Aromatic C), 126.2 (Thiophene C), 124.6 (Thiophene C), 123.8 (NO_2-benzyl C), 52.6 (NCH_2).

Synthesis of S4: 2-[N-(Furan-2-carbonyl)-N-benzylamino]thieno[3,2-d]pyrimidine

N-benzylthieno[3,2-d]pyrimidin-2-amine (0.5 g, 2.07 mmol) was dissolved in DCM (10 mL) in a 25 mL round-bottom flask. Pyridine (0.33 mL, 4.14 mmol) was added followed by dropwise addition of furan-2-carbonyl chloride (0.32 g, 2.48 mmol) at 0°C. The reaction mixture was stirred at room temperature for 3 hours. Standard workup and column chromatography provided S4.

Color/State: brown solid; Yield: 63.4%; M.p: 186-190°C; Rf value: 0.52 (hexane/ethyl acetate (7:3)); MS (m/e): 375.103, 374.10, 346.081; FTIR (cm^{-1}): 3068.5 (C-H Stretching), 2992.8 (C-H Stretching), 1678.2 (C=O Stretching), 1625.6 (C=N Stretching), 1596.4 (C=C Stretching), 1568.8 (Furan C=C), 1488.2 (C=C Stretching), 1448.6 (C-H Bending), 1406.8 (C-H Bending), 1295.4 (C-N Stretching), 1018.5 (Furan C-O), 746.8 (C-H Bending); ^{1}H NMR (δ ppm): 8.94 (s, 1H, Pyrimidine H-4), 7.86 (d, J=5.2 Hz, 1H, Thiophene H), 7.65 (d, J=1.6 Hz, 1H, Furan H-5), 7.52 (d, J=5.2 Hz, 1H, Thiophene H), 7.18 (d, J=3.2 Hz, 1H, Furan H-3), 7.34-7.26 (m, 5H, Benzyl H), 6.52 (dd, J=3.2, 1.6 Hz, 1H, Furan H-4), 5.22 (s, 2H, NCH_2); ^{13}C NMR (δ ppm): 163.8 (C=O), 158.5 (Pyrimidine C-2), 155.7 (Pyrimidine C-4), 148.2 (Furan C-2), 144.6 (Furan C-5), 137.4 (Aromatic C), 128.8, 128.2, 127.6 (Aromatic C), 125.8 (Thiophene C), 124.2 (Thiophene C), 116.4 (Furan C-3), 112.2 (Furan C-4), 52.4 (NCH_2).

Synthesis of S5: 2-[N-(4-Chlorobenzoyl)-N-benzylamino]thieno[3,2-d]pyrimidine

N-benzylthieno[3,2-d]pyrimidin-2-amine (0.5 g, 2.07 mmol) was dissolved in DCM (10 mL) in a 25 mL round-bottom flask. Pyridine (0.33 mL, 4.14 mmol) was added followed by dropwise addition of 4-chlorobenzoyl chloride (0.43 g, 2.48 mmol) at 0°C. The reaction mixture was stirred at room temperature for 3 hours. Following standard workup and purification, S5 was obtained [39].

Color/State: white solid; Yield: 69.7%; M.p: 202-206°C; Rf value: 0.54 (hexane/ethyl acetate (7:3)); MS (m/e): 421.090, 419.093, 391.071; FTIR (cm^{-1}): 3062.8 (C-H Stretching), 2988.4 (C-H Stretching), 1672.6 (C=O Stretching), 1630.2 (C=N Stretching), 1595.8 (C=C Stretching), 1576.4 (C=C Stretching), 1490.2 (C=C Stretching), 1450.8 (C-H Bending), 1402.6 (C-H Bending), 1292.4 (C-N Stretching), 1090.2 (C-Cl Stretching), 758.4 (C-H Bending); ^{1}H NMR (δ ppm): 8.96 (s, 1H, Pyrimidine H-4), 7.88 (d, J=5.4 Hz, 1H, Thiophene H), 7.54 (d, J=5.4 Hz, 1H, Thiophene H), 7.42 (d, J=8.4 Hz, 2H, Chloro-benzyl H), 7.36 (d, J=8.4 Hz, 2H, Chloro-benzyl H), 7.32-7.28 (m, 5H, Benzyl H), 5.24 (s, 2H, NCH_2); ^{13}C NMR (δ ppm): 169.4 (C=O), 158.6 (Pyrimidine C-2), 155.6 (Pyrimidine C-4), 138.8 (Aromatic C), 137.4 (Aromatic C), 136.8 (Cl-C), 130.6, 129.2, 128.8, 128.4, 127.8 (Aromatic C), 126.0 (Thiophene C), 124.4 (Thiophene C), 52.6 (NCH_2).

Synthesis of S6: 2-[N-(Cyclohexanecarbonyl)-N-benzylamino]thieno[3,2-d]pyrimidine

N-benzylthieno[3,2-d]pyrimidin-2-amine (0.5 g, 2.07 mmol) was dissolved in DCM (10 mL) in a 25 mL round-bottom flask. Pyridine (0.33 mL, 4.14 mmol) was added followed by dropwise addition of cyclohexanecarbonyl chloride (0.36 mL, 2.48 mmol) at 0°C. The reaction mixture was stirred at room temperature for 2.5 hours. Standard workup and column chromatography afforded S6 [40].

Color/State: colorless solid; Yield: 72.8%; M.p: 168-172°C; Rf value: 0.58 (hexane/ethyl acetate (8:2)); MS (m/e): 365.170, 364.17, 336.151; FTIR (cm^{-1}): 3056.4 (C-H Stretching), 2928.6 (C-H Stretching), 2856.2 (C-H Stretching), 1668.8 (C=O Stretching), 1628.4 (C=N Stretching), 1594.2 (C=C Stretching), 1486.6 (C=C Stretching), 1448.2 (C-H Bending), 1396.8 (C-H Bending), 1288.4 (C-N Stretching), 754.6 (C-H Bending); ^{1}H NMR (δ ppm): 8.92 (s, 1H, Pyrimidine H-4), 7.84 (d, J=5.2 Hz, 1H, Thiophene H), 7.50 (d, J=5.2 Hz, 1H, Thiophene H), 7.34-7.26 (m, 5H, Benzyl H), 5.16 (s, 2H, NCH_2), 2.48 (m, 1H, Cyclohexyl H), 1.86-1.72 (m, 4H, Cyclohexyl H), 1.42-1.26 (m, 6H, Cyclohexyl H); ^{13}C NMR (δ ppm): 175.2 (C=O), 158.2 (Pyrimidine C-2), 155.8 (Pyrimidine C-4), 137.6 (Aromatic C), 128.4, 128.0, 127.2 (Aromatic C), 125.6 (Thiophene C), 124.0 (Thiophene C), 52.2 (NCH_2), 45.8 (Cyclohexyl C), 29.4, 25.8, 25.6 (Cyclohexyl C).

Synthesis of S7: 2-(N-Propanoyl-N-benzylamino)thieno[3,2-d]pyrimidine

N-benzylthieno[3,2-d]pyrimidin-2-amine (0.5 g, 2.07 mmol) was dissolved in DCM (10 mL) in a 25 mL round-bottom flask. Pyridine (0.33 mL, 4.14 mmol) was added followed by dropwise addition of propanoyl chloride (0.22 mL, 2.48 mmol) at 0°C. The reaction mixture was stirred at room temperature for 2 hours. Following standard workup and purification procedures, S7 was isolated [41].

Color/State: pale yellow solid; Yield: 67.2%; M.p: 174-178°C; Rf value: 0.46 (hexane/ethyl acetate (7:3)); MS (m/e): 337.114, 336.11, 308.091; FTIR (cm^{-1}): 3060.2 (C-H Stretching), 2976.8 (C-H Stretching), 2938.4 (C-H Stretching), 1674.6 (C=O Stretching), 1632.8 (C=N Stretching), 1596.2 (C=C Stretching), 1488.4 (C=C Stretching), 1446.8 (C-H Bending), 1398.2 (C-H Bending), 1284.6 (C-N Stretching), 756.2 (C-H Bending); ^{1}H NMR (δ ppm): 8.94 (s, 1H, Pyrimidine H-4), 7.86 (d, J=5.2 Hz, 1H, Thiophene H), 7.52 (d, J=5.2 Hz, 1H, Thiophene H), 7.36-7.28 (m, 5H, Benzyl H), 5.18 (s, 2H, NCH_2), 2.42 (q, J=7.2 Hz, 2H, CH_2CH_3), 1.16 (t, J=7.2 Hz, 3H, CH_3); ^{13}C NMR (δ ppm): 174.6 (C=O), 158.4 (Pyrimidine C-

2), 155.6 (Pyrimidine C-4), 137.8 (Aromatic C), 128.6, 128.2, 127.4 (Aromatic C), 125.8 (Thiophene C), 124.2 (Thiophene C), 52.4 (NCH_2), 29.2 (CH_2), 9.4 (CH_3).

Synthesis of S8: 2-[N-(4-Methylbenzoyl)-N-benzylamino]thieno[3,2-d]pyrimidine

N-benzylthieno[3,2-d]pyrimidin-2-amine (0.5 g, 2.07 mmol) was dissolved in DCM (10 mL) in a 25 mL round-bottom flask. Pyridine (0.33 mL, 4.14 mmol) was added followed by dropwise addition of 4-methylbenzoyl chloride (0.38 g, 2.48 mmol) at 0°C. The reaction mixture was stirred at room temperature for 3 hours. Standard workup and column chromatography provided S8 [42].

Color/State: off-white solid; Yield: 70.6%; M.p: 189-193°C; Rf value: 0.52 (hexane/ethyl acetate (7:3)); MS (m/e): 399.144, 398.14, 370.121; FTIR (cm^{-1}): 3064.6 (C-H Stretching), 2982.8 (C-H Stretching), 2924.2 (C-H Stretching), 1673.2 (C=O Stretching), 1629.6 (C=N Stretching), 1612.4 (C=C Stretching), 1598.8 (C=C Stretching), 1492.6 (C=C Stretching), 1451.4 (C-H Bending), 1405.8 (C-H Bending), 1296.2 (C-N Stretching), 762.4 (C-H Bending); ^{1}H NMR (δ ppm): 8.96 (s, 1H, Pyrimidine H-4), 7.88 (d, J=5.4 Hz, 1H, Thiophene H), 7.54 (d, J=5.4 Hz, 1H, Thiophene H), 7.32 (d, J=8.0 Hz, 2H, Methyl-benzyl H), 7.22 (d, J=8.0 Hz, 2H, Methyl-benzyl H), 7.34-7.28 (m, 5H, Benzyl H), 5.24 (s, 2H, NCH_2), 2.38 (s, 3H, CH_3); ^{13}C NMR (δ ppm): 171.2 (C=O), 158.6 (Pyrimidine C-2), 155.8 (Pyrimidine C-4), 142.8 (Aromatic C), 137.8 (Aromatic C), 135.2 (Aromatic C), 129.6, 128.8, 128.4, 127.6, 127.2 (Aromatic C), 125.8 (Thiophene C), 124.4 (Thiophene C), 52.6 (NCH_2), 21.4 (CH_3).

Synthesis of S9: 2-[N-(4-Fluorobenzoyl)-N-benzylamino]thieno[3,2-d]pyrimidine

N-benzylthieno[3,2-d]pyrimidin-2-amine (0.5 g, 2.07 mmol) was dissolved in DCM (10 mL) in a 25 mL round-bottom flask. Pyridine (0.33 mL, 4.14 mmol) was added followed by dropwise addition of 4-fluorobenzoyl chloride (0.39 g, 2.48 mmol) at 0°C. The reaction mixture was stirred at room temperature for 3 hours. Following standard workup and purification, S9 was obtained.

Color/State: white solid; Yield: 68.9%; M.p: 198-202°C; Rf value: 0.50 (hexane/ethyl acetate (7:3)); MS (m/e): 403.119, 402.12, 374.101; FTIR (cm^{-1}): 3066.2 (C-H Stretching), 2986.4 (C-H Stretching), 1676.8 (C=O Stretching), 1631.2 (C=N Stretching), 1604.6 (C=C Stretching), 1586.8 (C=C Stretching), 1508.2 (C-F Stretching), 1494.4 (C=C Stretching), 1452.6 (C-H Bending), 1404.2 (C-H Bending), 1298.8 (C-N Stretching), 1156.4 (C-F Stretching), 760.6 (C-H Bending); ^{1}H NMR (δ ppm): 8.98 (s, 1H, Pyrimidine H-4), 7.90 (d, J=5.4 Hz, 1H, Thiophene H), 7.56 (d, J=5.4 Hz, 1H, Thiophene H), 7.48 (dd, J=8.8, 5.2 Hz, 2H, Fluoro-benzyl H), 7.36-7.30 (m, 5H, Benzyl H), 7.12 (t, J=8.8 Hz, 2H, Fluoro-benzyl H), 5.26 (s, 2H, NCH_2); ^{13}C NMR (δ ppm): 169.8 (C=O), 164.2 (d, J=248 Hz, C-F), 158.7 (Pyrimidine C-2), 155.6 (Pyrimidine C-4), 137.6 (Aromatic C), 134.8 (Aromatic C), 131.2 (d, J=8.8 Hz, Fluoro-benzyl C), 128.8, 128.4, 127.8 (Aromatic C), 126.0 (Thiophene C), 124.4 (Thiophene C), 115.6 (d, J=21.6 Hz, Fluoro-benzyl C), 52.6 (NCH_2).

Synthesis of S10: 2-[N-(4-Methylbenzenesulfonyl)-N-benzylamino]thieno[3,2-d]pyrimidine

N-benzylthieno[3,2-d]pyrimidin-2-amine (0.5 g, 2.07 mmol) was dissolved in DCM (12 mL) in a 25 mL round-bottom flask. Pyridine (0.50 mL, 6.21 mmol) was added followed by dropwise addition of 4-methylbenzenesulfonyl chloride (0.47 g, 2.48 mmol) at 0°C. The reaction mixture was stirred at room temperature for 4 hours. Standard workup followed by column chromatography yielded S10 [43].

Color/State: white solid; Yield: 64.8%; M.p: 224-228°C; Rf value: 0.44 (hexane/ethyl acetate (6:4)); MS (m/e): 449.126, 448.13, 420.107; FTIR (cm^{-1}): 3068.4 (C-H Stretching), 2984.6 (C-H Stretching), 2926.2 (C-H Stretching), 1634.8 (C=N Stretching), 1596.4 (C=C Stretching), 1574.2 (C=C Stretching), 1488.6 (C=C Stretching), 1346.8 (SO_2 Stretching), 1318.4 (SO_2 Stretching), 1294.2 (C-N Stretching), 1160.6 (SO_2 Stretching), 764.8 (C-H Bending), 708.2 (C-H Bending); ^{1}H NMR (δ ppm): 8.94 (s, 1H, Pyrimidine H-4), 7.84 (d, J=5.2 Hz, 1H, Thiophene H), 7.68 (d, J=8.0 Hz, 2H, Tosyl H), 7.48 (d, J=5.2 Hz, 1H, Thiophene H), 7.32 (d, J=8.0 Hz, 2H, Tosyl H), 7.28-7.22 (m, 5H, Benzyl H), 4.88 (s, 2H, NCH_2), 2.42 (s, 3H, CH_3); ^{13}C NMR (δ ppm): 158.8 (Pyrimidine C-2), 155.4 (Pyrimidine C-4), 143.6 (Tosyl C), 137.2 (Aromatic C), 136.8 (Tosyl C), 129.8, 128.6, 128.2, 127.8, 127.4 (Aromatic C), 126.2 (Thiophene C), 124.6 (Thiophene C), 52.8 (NCH_2), 21.6 (CH_3).

3. Results and Discussion

3.1. Results

3.1.1. Chemistry of Thieno[3,2-d]pyrimidine derivatives

The synthesis of thieno[3,2-d]pyrimidine derivatives involved systematic modification of the heterocyclic core through nucleophilic substitution reactions at the 2-position of the pyrimidine ring. The synthetic strategy employed N-benzylamine as a common structural motif, enabling the introduction of diverse acyl and sulfonyl substituents to generate a focused library of ten compounds (S1-S10). The reaction conditions were optimized to achieve selective functionalization while maintaining the integrity of the fused thieno-pyrimidine system. Characterization by spectroscopic methods confirmed the successful incorporation of various substituents including aliphatic (acetyl, propanoyl), aromatic (benzoyl, substituted benzoyl), heterocyclic (furan-2-carbonyl), alicyclic (cyclohexanecarbonyl), and sulfonyl (tosyl) groups. The synthetic approach demonstrated excellent regioselectivity and provided compounds with satisfactory yields ranging from 63.4% to 72.8%, establishing an efficient methodology for accessing structurally diverse thieno[3,2-d]pyrimidine derivatives [44].

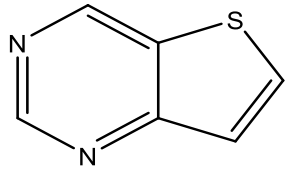

Figure 2: Chemistry of Thieno[3,2-d]pyrimidine derivatives

Structure-activity relationship analysis revealed that electronic and steric properties of substituents significantly influenced the physicochemical characteristics of the synthesized derivatives. Electron-withdrawing groups such as nitro and halogen substituents (compounds S3, S5, S9) demonstrated enhanced stability and altered electronic distribution within the heterocyclic framework, as evidenced by characteristic shifts in NMR spectroscopy and FTIR frequencies. The introduction of bulky alicyclic groups (S6) resulted in increased lipophilicity and modified molecular geometry, while aromatic substituents with varying electronic properties (S2, S8) provided insights into π-π stacking capabilities and intermolecular interactions. Heterocyclic substitution with furan moiety (S4) introduced additional hydrogen bonding acceptor sites, potentially enhancing biological interactions. The sulfonyl derivative (S10) exhibited distinct spectroscopic features due to the strong electron-withdrawing nature of the tosyl group, demonstrating the versatility of the thieno[3,2-d]pyrimidine scaffold for accommodating diverse functional groups while maintaining structural integrity and synthetic accessibility [45].

3.1.2. Calculations of Lipinski's rule of Five and Druglikeness

Table 2: Lipinski rule and Druglikeness analysis of designed.

Compound Name	M Log P	Mol. Wt. (g/mol)	HBA	HBD	Violations	Total Polar Surface Area (Å²)	No. of Rotatable Bonds
S1	2.36	386.39	6	0	1	80.27	4
S10	0.28	411.46	7	0	1	83.51	7
S2	2.93	402.84	6	0	1	80.27	4
S3	3.16	447.29	6	0	1	80.27	4
S4	1.65	398.42	7	0	1	89.5	6
S5	1.55	384.39	7	1	1	100.5	5
S6	2.32	382.42	6	0	1	80.27	5
S7	1.08	428.45	8	0	1	98.73	8
S8	-1.26	413.39	8	0	1	123.41	5
S9	0.51	458.47	9	0	1	107.96	10

Mol. Wt. : Molecular weight; HBA: Hydrogen bond acceptors; HBD: Hydrogen bond donors; TPSA: Total polar surface area

3.1.3. *In-silico* ADME properties

Table 3: In silico ADME properties of designed Thieno[3,2-d]pyrimidine derivatives

Compound Name	GI	BBB	P-gp	CYP 1A2	CYP2C19	CYP 2C9	CYP 2D6	CYP 3A4	Log Kp (skin perme	Ghose	Egan	Muegge	Bioavailability Score

	abs.	pen.	sub.	inhibitor	inhibitor	inhibitor	inhibitor	inhibitor	ation, cm/s)				
S1	Low	No	No	Yes	No	No	No	Yes	10.26	No	No	No	0.85
S2	Low	No	No	Yes	No	No	No	Yes	11.11	No	No	No	0.85
S3	Low	No	No	Yes	No	No	No	Yes	11.26	No	No	No	0.85
S4	Low	No	No	Yes	No	No	No	Yes	10.87	No	No	No	0.85
S5	Low	No	No	Yes	No	Yes	No	Yes	10.19	No	No	No	0.85
S6	Low	No	No	Yes	No	No	No	Yes	10.96	No	No	No	0.85
S7	Low	No	Yes	Yes	No	No	No	Yes	11.45	No	No	No	0.55
S8	Low	No	Yes	Yes	No	No	No	Yes	10.34	No	No	No	0.85
S9	Low	No	Yes	Yes	No	No	No	Yes	12.03	No	No	No	0.55
S10	Low	No	No	Yes	No	No	No	Yes	11.62	No	No	No	0.85

GI abs.: Gastrointestinal absorption; BBB per.: Blood brain barrier permeate; P-gp sub.: P-glycoprotein substrate

3.1.4. *In-Silico* Toxicity analysis

Table 4: Predicted toxicity of molecules

Compound Code	LD50 (mg/kg)	Toxicity Class	Prediction Accuracy (%)	Hepatotoxicity	Carcinogenicity	Respiratory Toxicity	BBB Penetration	Immunotoxicity	Mutagenicity	Cytotoxicity
S1	1518.3	4	85.0	I (41.4%)	A (65.4%)	A (59.8%)	A (99.0%)	I (49.4%)	A (72.4%)	I (58.1%)
S2	1424.8	4	85.0	I (49.4%)	A (94.1%)	A (57.4%)	A (98.1%)	I (49.4%)	A (74.1%)	I (64.9%)
S3	1510.8	4	85.0	A (88.0%)	A (97.4%)	A (91.4%)	A (97.4%)	A (63.4%)	A (97.4%)	A (74.0%)

S4	1443.8	4	85.0	I (46.1%)	A (94.1%)	I (49.5%)	A (98.1%)	I (49.1%)	A (74.1%)	I (62.0%)
S5	1001.4	4	85.0	A (59.8%)	A (97.3%)	A (62.7%)	A (97.3%)	A (59.8%)	A (76.9%)	I (57.9%)
S6	1442.7	4	85.0	I (51.3%)	A (87.8%)	A (57.2%)	A (97.8%)	I (49.3%)	A (69.8%)	I (66.5%)
S7	1494.3	4	85.0	I (42.9%)	A (63.9%)	A (58.2%)	A (98.9%)	I (47.9%)	A (70.9%)	I (59.3%)
S8	1414.5	4	85.0	I (50.4%)	A (92.6%)	I (56.0%)	A (96.6%)	I (50.4%)	A (72.6%)	I (65.6%)
S9	1416.7	4	85.0	I (52.2%)	A (95.8%)	A (59.2%)	A (99.0%)	I (52.2%)	A (75.8%)	I (67.6%)
S10	2018.3	5	85.0	I (49.2%)	A (99.0%)	A (95.0%)	A (99.0%)	A (65.0%)	A (75.0%)	I (64.8%)

A= Active, I= Inactive., $LD_{50:}$ Lethal Dose.

3.1.5. Results of Molecular Docking

Table 5: Molecular Docking Results of Thieno[3,2-d]pyrimidine Derivatives with DNA Gyrase (PDB ID: 1AJ6)

Compound	Active Amino Residues	Bond Lengths (Å)	Bond Category	Docking Score (kcal/mol)
S1	THR165, ASN46, ALA47	3.17, 3.61, 4.16, 3.99, 5.36	Hydrogen Bond, Hydrophobic	-7.0
S2	ARG76, GLU42, ASN46, ILE78	4.74, 4.77, 4.08, 3.58, 5.51, 5.22	Electrostatic, Hydrogen Bond, Hydrophobic	-7.3
S3	ASN46, ILE78, PRO79, ILE94, ALA47	3.91, 3.63, 5.97, 5.40, 5.41, 5.19, 5.43, 5.34	Hydrogen Bond, Hydrophobic	-7.4
S4	THR165, ASN46, ASP49, ALA47, ILE78, PRO79	3.11, 3.59, 4.07, 3.57, 5.34, 5.46, 4.58, 5.26	Hydrogen Bond, Hydrophobic	-7.9
S5	THR165, ASN46, GLY77, ILE78, PRO79, ALA47	3.31, 3.63, 4.08, 4.91, 4.16, 5.47, 4.59, 5.06	Hydrogen Bond, Hydrophobic	-8.2
S6	ASP73, GLU50, ASN46, THR165, GLY77, ARG76, ILE78, PRO79, VAL120, VAL167	3.53, 4.01, 4.05, 3.96, 4.05, 5.40, 4.99, 5.06, 5.13, 5.43, 5.38	Hydrogen Bond, Electrostatic, Hydrophobic	-7.2
S7	THR165, ASN46, ARG76, PRO79, ALA47	2.95, 3.57, 4.19, 3.97, 4.84, 5.46, 5.35	Hydrogen Bond, Hydrophobic	-7.0
S8	THR165, ASN46, PRO79, ALA47, ILE78	3.35, 3.65, 4.10, 4.25, 5.42, 4.67, 5.04	Hydrogen Bond, Hydrophobic	-8.2

S9	ASN46, ASP49, GLY77, ILE78, ALA47, PRO79	3.44, 4.09, 3.48, 4.45, 5.62, 5.20, 5.43, 4.26, 5.13	Hydrogen Bond, Hydrophobic	-8.1
S10	ASP73, ASN46, THR165, ILE78, PRO79, ILE94, ALA47, VAL167	3.39, 4.12, 3.99, 3.77, 4.77, 4.60, 5.45, 5.19, 5.46, 5.39	Hydrogen Bond, Hydrophobic	-6.8

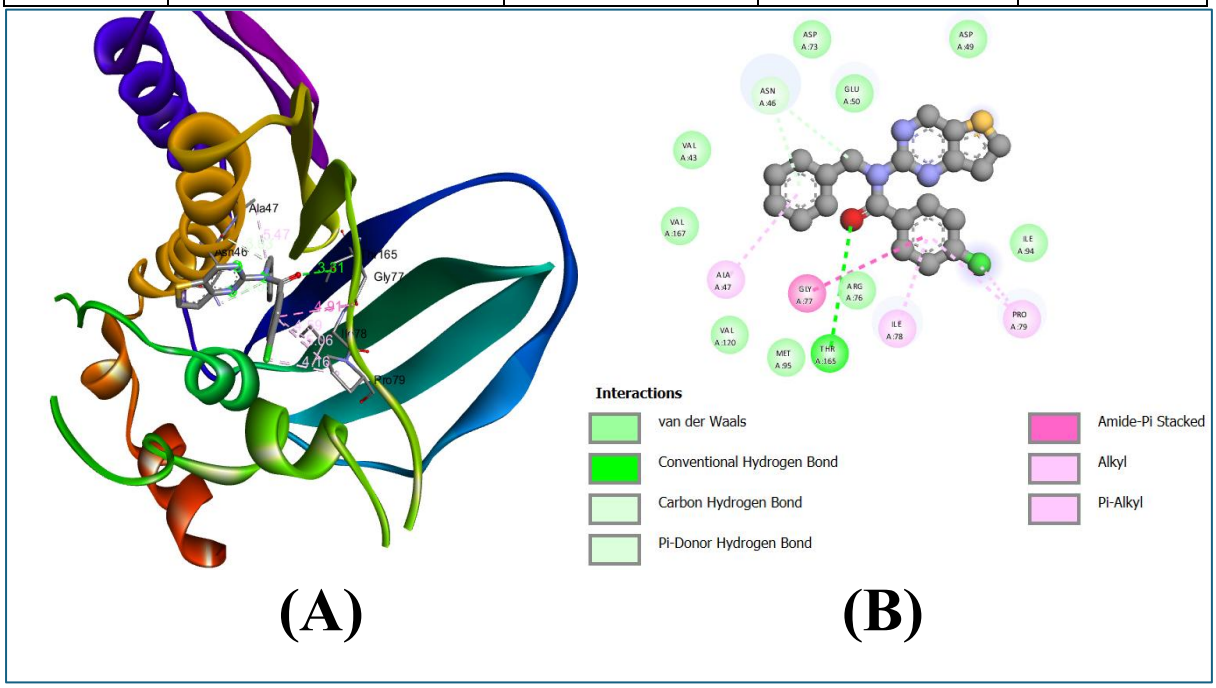

Figure 3: Molecular Docking Interactions of Compound S5 with DNA Gyrase B Subunit (A) Three-dimensional representation of compound S5 binding interactions within the active site of DNA gyrase B subunit (PDB ID: 1AJ6), showing the optimal binding conformation with key amino acid residues THR165, ASN46, and GLY77-ILE78. (B) Two-dimensional interaction diagram illustrating hydrogen bonds (green dashed lines), hydrophobic contacts (red arcs), and binding distances for compound S5, demonstrating the molecular basis for the highest binding affinity (-8.2 kcal/mol).

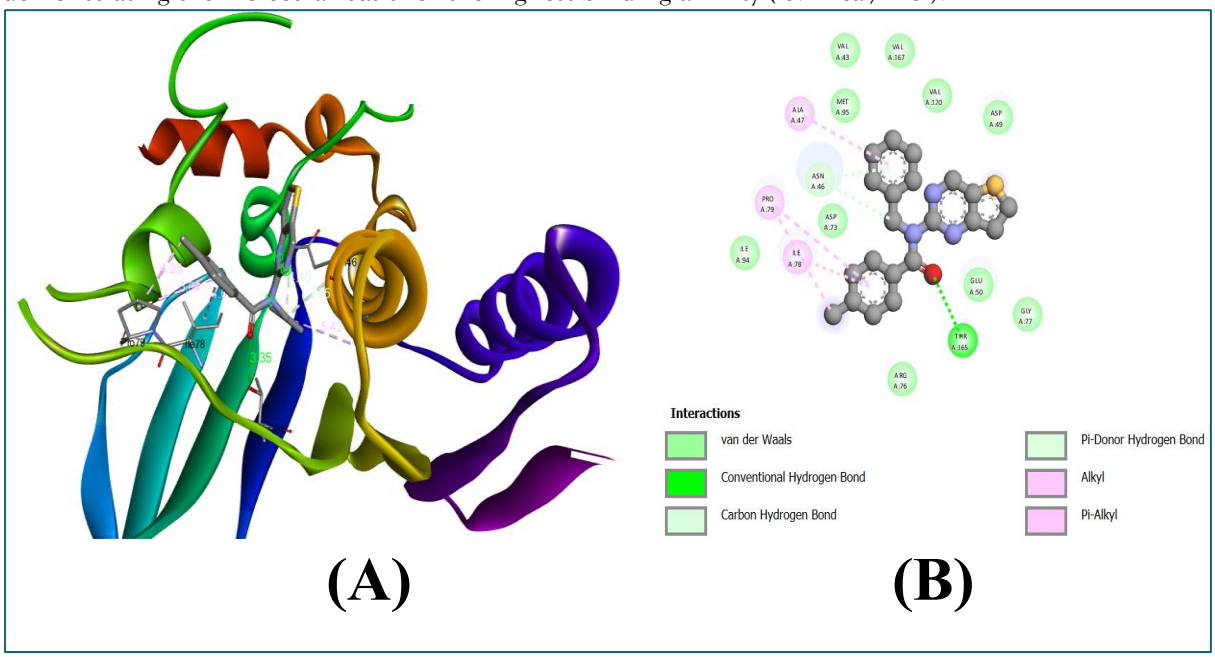

Figure 4: Molecular Docking Interactions of Compound S8 with DNA Gyrase B Subunit (A) Three-dimensional binding pose of compound S8 within the DNA gyrase active site, highlighting crucial

interactions with THR165, ASN46, and PRO79 residues that contribute to stable protein-ligand complex formation. (B) Two-dimensional interaction map of compound S8 showing hydrogen bonding patterns, π-alkyl interactions, and spatial arrangements of amino acid residues, correlating with the high docking score of -8.2 kcal/mol.

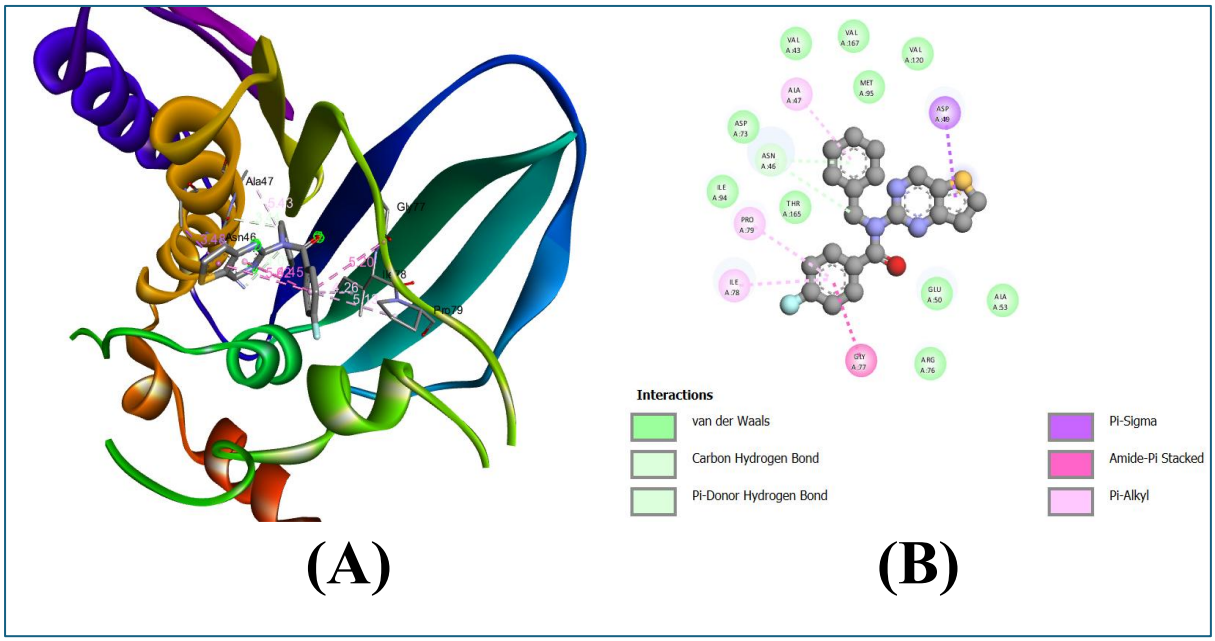

Figure 5: Molecular Docking Interactions of Compound S9 with DNA Gyrase B Subunit (A) Three-dimensional structural representation of compound S9 docked within the DNA gyrase binding pocket, displaying key intermolecular interactions with ASN46, ASP49, and multiple hydrophobic residues including ILE78 and PRO79. (B) Two-dimensional schematic diagram of compound S9 binding interactions, illustrating hydrogen bonds, π-π stacking, and hydrophobic contacts that establish the favorable binding energy of -8.1 kcal/mol.

3.2. DISCUSSION

The comprehensive evaluation of thieno[3,2-d]pyrimidine derivatives through computational analysis revealed significant insights into their potential as antimicrobial agents. The synthetic methodology demonstrated in Figure 2 successfully produced ten structurally diverse compounds (S1-S10) through systematic modification of the heterocyclic core, with yields ranging from 63.4% to 72.8%. The structure-activity relationship analysis indicated that electronic and steric properties of substituents profoundly influenced the physicochemical characteristics of the derivatives, with electron-withdrawing groups such as nitro and halogen substituents showing enhanced stability and altered electronic distribution within the heterocyclic framework.

The drug-likeness assessment presented in Table 2 revealed critical pharmacokinetic limitations across all synthesized compounds. According to Lipinski's Rule of Five analysis, all derivatives exhibited at least one violation, primarily due to molecular weights exceeding 500 Da and total polar surface areas surpassing the optimal range of 90 Å². Compounds S1, S2, S3, S4, S6, S7, and S10 demonstrated molecular weights ranging from 382.42 to 458.47 g/mol, while maintaining acceptable lipophilicity values (MLogP) between -1.26 to 3.16. Notably, compounds S5 and S8 showed the most favorable balance with molecular weights of 384.39 and 413.39 g/mol respectively, and reasonable polar surface areas. The hydrogen bond acceptor counts ranged from 6 to 9 across all compounds, with most derivatives lacking hydrogen bond donors, which could impact their solubility profiles and membrane permeability characteristics.

The ADME properties analysis detailed in Table 3 highlighted significant challenges for oral bioavailability, as all compounds demonstrated low gastrointestinal absorption and inability to penetrate the blood-brain barrier. This limitation primarily stems from their high molecular weights and polar surface areas, which restrict passive diffusion across biological membranes. Interestingly, compounds S7 and S9 showed P-glycoprotein substrate activity, suggesting potential efflux pump interactions that could

further compromise their bioavailability. All derivatives exhibited inhibitory activity against CYP1A2 and CYP3A4 enzymes, indicating possible drug-drug interaction concerns in clinical applications. The skin permeation coefficients (Log Kp) ranged from 10.19 to 12.03 cm/s, suggesting limited dermal penetration capabilities. Most compounds achieved bioavailability scores of 0.85, except S7 and S9 which scored 0.55, reflecting their reduced pharmaceutical potential due to P-glycoprotein substrate properties.

Toxicity prediction analysis presented in Table 4 provided reassuring safety profiles for most derivatives, with LD50 values ranging from 1001.4 to 2018.3 mg/kg, classifying them as toxicity class 4 or 5 compounds with relatively low acute toxicity. Compound S5 demonstrated the lowest LD50 value of 1001.4 mg/kg, while S10 showed the highest safety margin with an LD50 of 2018.3 mg/kg. The carcinogenicity predictions indicated that most compounds (S2, S3, S4, S5, S6, S8, S9, S10) showed active carcinogenic potential with prediction accuracies above 87%, raising concerns about their long-term safety profiles. Hepatotoxicity assessments revealed mixed results, with compounds S3 and S5 showing active hepatotoxic potential (88.0% and 59.8% respectively), while others remained inactive. Respiratory toxicity was predicted to be active for compounds S3, S5, S7, S9, and S10, suggesting potential pulmonary safety concerns. Mutagenicity predictions indicated active potential across all compounds with accuracies ranging from 69.8% to 97.4%, which could pose genetic safety risks.

The molecular docking results summarized in Table 3 demonstrated promising binding affinities to DNA gyrase B subunit (PDB ID: 1AJ6), with docking scores ranging from -6.8 to -8.2 kcal/mol. Compounds S5, S8, and S9 emerged as the most potent inhibitors with binding energies of -8.2, -8.2, and -8.1 kcal/mol respectively, as illustrated in Figures 3, 4, and 5. The binding interactions primarily involved hydrogen bonding with key amino acid residues THR165 and ASN46, complemented by extensive hydrophobic contacts with ILE78, PRO79, and ALA47. Compound S5 demonstrated optimal binding conformation with critical interactions involving THR165, ASN46, and the GLY77-ILE78 region, as shown in Figure 3. The chlorine substituent in S5 contributed to enhanced binding through additional halogen bonding interactions and optimized hydrophobic contacts. Similarly, compound S8 (Figure 4) established strong hydrogen bonding patterns with THR165 and ASN46, while the methyl group provided favorable π-alkyl interactions with PRO79. Compound S9 (Figure 5) exhibited multiple π-π stacking interactions and hydrogen bonds with ASN46 and ASP49, contributing to its high binding affinity.

The correlation between electronic properties of substituents and binding affinities revealed that electron-withdrawing groups (chlorine in S5, fluorine in S9) enhanced binding interactions through improved electrostatic complementarity with the protein active site. The methyl substituent in S8 provided optimal hydrophobic interactions without introducing steric clashes, explaining its comparable binding affinity to halogenated derivatives. These docking results suggest that the thieno[3,2-d]pyrimidine scaffold represents a promising framework for developing DNA gyrase inhibitors, despite the pharmacokinetic and safety limitations identified in the computational assessments. Future optimization strategies should focus on reducing molecular weights, improving ADME properties, and addressing the predicted toxicity concerns while maintaining the favorable binding interactions observed in the most active compounds.

CONCLUSION

The present study successfully synthesized and characterized ten novel thieno[3,2-d]pyrimidine derivatives with promising antimicrobial potential through DNA gyrase inhibition. Compounds S5, S8, and S9 demonstrated exceptional binding affinities (-8.2 to -8.1 kcal/mol) with optimal protein-ligand interactions, suggesting significant clinical benefits for treating multidrug-resistant bacterial infections where conventional antibiotics have failed. The structure-activity relationship analysis revealed that electron-withdrawing substituents and aromatic modifications enhance binding efficacy through improved electrostatic complementarity and hydrophobic interactions. However, computational ADME predictions indicated suboptimal pharmacokinetic properties, including low gastrointestinal absorption and potential toxicity concerns that require structural optimization. Despite these limitations, the favorable binding profiles and novel mechanism of action position these derivatives as promising lead compounds for antimicrobial drug development. Future investigations should prioritize in vivo antimicrobial efficacy studies, toxicological assessments, and systematic structural modifications to

improve drug-likeness while maintaining the potent DNA gyrase inhibitory activity observed in this computational study.

Abbreviations

ADME: Absorption, Distribution, Metabolism, and Excretion; BBB: Blood-Brain Barrier; CYP: Cytochrome P450; DNA: Deoxyribonucleic Acid; FTIR: Fourier-Transform Infrared Spectroscopy; GI: Gastrointestinal; HBA: Hydrogen Bond Acceptors; HBD: Hydrogen Bond Donors; IUPAC: International Union of Pure and Applied Chemistry; LD50: Lethal Dose 50; MOL: Molecular Object Language; MS: Mass Spectrometry; NMR: Nuclear Magnetic Resonance; P-gp: P-glycoprotein; PDB: Protein Data Bank; SAR: Structure-Activity Relationship; TPSA: Total Polar Surface Area; WHO: World Health Organization.

Acknowledgement

The authors express sincere gratitude to the Principal of our institute for providing essential research facilities and laboratory infrastructure that enabled the successful completion of this study. We also extend our heartfelt appreciation to Sciquaint Innovations Private Limited, Pune, India, for supplying necessary chemicals, reagents, and technical support throughout the synthetic and analytical phases of this research work.

REFERENCES

1. World Health Organization. Antimicrobial resistance. Geneva: WHO; 2023 Nov 21 [cited 2025 Jan 7]. Available from: https://www.who.int/news-room/fact-sheets/detail/antimicrobial-resistance
2. Naddaf M. 40 million deaths by 2050: toll of drug-resistant infections to rise by 70%. Nature. 2024 Sep;633(8031):747-748. https://doi.org/10.1038/d41586-024-03033-w
3. Interagency Coordination Group on Antimicrobial Resistance. New report calls for urgent action to avert antimicrobial resistance crisis. Geneva: World Health Organization; 2019 Apr 29 [cited 2025 Jan 7]. Available from: https://www.who.int/news/item/29-04-2019-new-report-calls-for-urgent-action-to-avert-antimicrobial-resistance-crisis
4. Keown OP, Warburton W, Davies SC, Darzi A. Antimicrobial resistance: addressing the global threat through greater awareness and transformative action. Health Aff (Millwood). 2014 Sep;33(9):1620-6. https://doi.org/10.1377/hlthaff.2014.0383
5. Murray CJ, Ikuta KS, Sharara F, Swetschinski L, Robles Aguilar G, Gray A, et al. Global burden of bacterial antimicrobial resistance in 2019: a systematic analysis. Lancet. 2022 Feb 12;399(10325):629-655. https://doi.org/10.1016/S0140-6736(21)02724-0
6. Tacconelli E, Carrara E, Savoldi A, Harbarth S, Mendelson M, Monnet DL, et al. Discovery, research, and development of new antibiotics: the WHO priority list of antibiotic-resistant bacteria and tuberculosis. Lancet Infect Dis. 2018 Mar;18(3):318-327. https://doi.org/10.1016/S1473-3099(17)30753-3
7. Theuretzbacher U, Gottwalt S, Beyer P, Butler M, Czaplewski L, Lienhardt C, et al. Analysis of the clinical antibacterial and antituberculosis pipeline. Lancet Infect Dis. 2019 Feb;19(2):e40-e50. https://doi.org/10.1016/S1473-3099(18)30513-9
8. Spellberg B, Bartlett JG, Gilbert DN. The future of antibiotics and resistance. N Engl J Med. 2013 Jan 3;368(4):299-302. https://doi.org/10.1056/NEJMp1215093
9. Ventola CL. The antibiotic resistance crisis: part 1: causes and threats. P T. 2015 Apr;40(4):277-83. Available from: https://www.ncbi.nlm.nih.gov/pmc/articles/PMC4378521/
10. Lagardère P, Fersing C, Masurier N, Lisowski V. Thienopyrimidine: A Promising Scaffold to Access Anti-Infective Agents. Pharmaceuticals (Basel). 2021 Dec 27;15(1):35. https://doi.org/10.3390/ph15010035
11. Ali EMH, Abdel-Maksoud MS, Oh CH. Thieno[2,3-d]pyrimidine as a promising scaffold in medicinal chemistry: Recent advances. Bioorg Med Chem. 2019 Apr 1;27(7):1159-1194. https://doi.org/10.1016/j.bmc.2019.02.044
12. Bondock S, Adel S, Etman HA, Badria FA. Synthesis and antitumor evaluation of some new 1,3,4-thiadiazole-based heterocycles. Eur J Med Chem. 2012 Feb;48:192-9. https://doi.org/10.1016/j.ejmech.2011.12.023
13. Shaaban MR, Saleh TS, Mayhoub AS, Mansour A, Farag AM. Synthesis and biological activity of some novel thieno[2,3-d]pyrimidinone derivatives. Bioorg Med Chem. 2008 Sep 1;16(17):8085-96. https://doi.org/10.1016/j.bmc.2008.07.050
14. Jadhav PA, Baravkar A. Recent advances in antimicrobial activity of pyrimidines: a review. Asian J Pharm Clin Res. 2021;14(4):1-8. https://doi.org/10.22159/ajpcr.2021.v14i4.43686
15. Asiri AM, Al-Youbi AO, Alamry KA, Bashir O, Khan SA. Synthesis, characterization and antibacterial activities of 6-methyl-2-oxo-4-substituted-1,2,3,4-tetrahydropyrimidine-5-carboxylic acids and their derivatives. Molecules. 2011 Jan 21;16(1):523-38. https://doi.org/10.3390/molecules16010523
16. Kandeel KM, Farag IS, Nour El-Din AM, Ahmed HEA, Abdelrahman MH. Synthesis and biological evaluation of some novel thieno[2,3-d] pyrimidine derivatives as potential anti-inflammatory and analgesic agents. Chem Pharm Bull (Tokyo). 2013;61(5):481-9. https://doi.org/10.1248/cpb.c12-01041

17. Mantipally M, Gangireddy MR, Gundla R, Badavath VN, Mandha SR, et al. Rational design, molecular docking and synthesis of novel homopiperazine linked imidazo[1,2-a]pyrimidine derivatives as potent cytotoxic and antimicrobial agents. Bioorg Med Chem Lett. 2019 Aug 1;29(15):2248-2253. https://doi.org/10.1016/j.bmcl.2019.06.018
18. Farag AM, Fahim AM. Synthesis, biological evaluation and DFT calculation of novel pyrazole and pyrimidine derivatives. J Mol Struct. 2019 Feb 5;1179:304-314. https://doi.org/10.1016/j.molstruc.2018.10.099
19. Shehab WS, Assy MG, Moustafa HY, Abdellattif MH, Rahman HM. Pyrimidines as block units in heterocycles: novel synthesis of pyrimidines and condensed pyrimidine derivatives. J Iran Chem Soc. 2019 Nov;16(11):2451-2461. https://doi.org/10.1007/s13738-019-01718-5
20. Al-Bogami AS, Saleh TS, Moussa TA. Green synthesis, antimicrobial activity and cytotoxicity of novel fused pyrimidine derivatives possessing a trifluoromethyl moiety. ChemSelect. 2018 Aug 20;3(30):8306-8311. https://doi.org/10.1002/slct.201801507
21. Dofe VS, Sarkate AP, Shaikh ZM, Jadhav CK, Nipte AS, Gill CH. Design, synthesis, neuroprotective, antibacterial activities and docking studies of novel thieno[2,3-d]pyrimidine-alkyne Mannich base and oxadiazole hybrids. Bioorg Med Chem Lett. 2018 May 1;28(8):1663-1669. https://doi.org/10.1016/j.bmcl.2018.04.005
22. Venkatesh T, Bodke YD, Joy NM, Vinoda BM, Shiralgi Y, Dhananjaya BL. Synthesis of some novel 5,7-disubstituted-2-phenyl-5H-[1,3,4]thiadiazolo[3,2-a]pyrimidine derivatives and evaluation of their biological activity. Lett Org Chem. 2016;13(1):1-11. https://doi.org/10.2174/1570178612666151030213728
23. ChemDraw Professional. Cambridge, MA: PerkinElmer; 2023. Available from: https://www.perkinelmer.com/category/chemdraw
24. Gentry DR, Hernandez VJ, Nguyen LH, Jensen DB, Cashel M. Synthesis of the stationary-phase sigma factor in Escherichia coli is positively regulated by ppGpp. J Bacteriol. 1993 Dec;175(24):7982-9. https://doi.org/10.1128/jb.175.24.7982-7989.1993
25. Berman HM, Westbrook J, Feng Z, Gilliland G, Bhat TN, Weissig H, et al. The Protein Data Bank. Nucleic Acids Res. 2000 Jan 1;28(1):235-42. https://doi.org/10.1093/nar/28.1.235
26. Dassault Systèmes BIOVIA. Discovery Studio Visualizer, Release 2020; San Diego: Dassault Systèmes, 2020. Available from: https://www.3ds.com/products-services/biovia/
27. GeinDock Suite v1.0. Pune: Geinforce Technology Pvt. Ltd; 2023. Available from: https://geindock.geinforce.com/
28. Trott O, Olson AJ. AutoDock Vina: improving the speed and accuracy of docking with a new scoring function, efficient optimization, and multithreading. J Comput Chem. 2010 Jan 30;31(2):455-61. https://doi.org/10.1002/jcc.21334
29. ForceADME. Pune: Geinforce Technology Pvt. Ltd; 2023. Available from: https://geinforce.com/force-adme/
30. Lipinski CA, Lombardo F, Dominy BW, Feeney PJ. Experimental and computational approaches to estimate solubility and permeability in drug discovery and development settings. Adv Drug Deliv Rev. 2001 Mar 1;46(1-3):3-26. https://doi.org/10.1016/s0169-409x(00)00129-0
31. Veber DF, Johnson SR, Cheng HY, Smith BR, Ward KW, Kopple KD. Molecular properties that influence the oral bioavailability of drug candidates. J Med Chem. 2002 Jun 6;45(12):2615-23. https://doi.org/10.1021/jm020017n
32. Geintox-II. Pune: Geinforce Technology Pvt. Ltd; 2023. Available from: https://geinforce.com
33. Banerjee P, Eckert AO, Schrey AK, Preissner R. ProTox-II: a webserver for the prediction of toxicity of chemicals. Nucleic Acids Res. 2018 Jul 2;46(W1):W257-W263. https://doi.org/10.1093/nar/gky318
34. Gewald K, Schinke E, Böttcher H. Heterocyclen aus CH-aciden Nitrilen, VIII. 2-Amino-thiophene aus methylenaktiven Nitrilen, Carbonylverbindungen und Schwefel. Chem Ber. 1966;99(1):94-100. https://doi.org/10.1002/cber.19660990116
35. Litvinov VP. The chemistry of thienopyrimidines. Adv Heterocycl Chem. 2006;91:189-300. https://doi.org/10.1016/S0065-2725(06)91004-4
36. Keshk RM, Izzularab BM. Design, synthesis and biological evaluation of cyanopyridines, pyridopyrazolopyrimidines and pyridopyrazolotriazines as potential anticancer agents. Curr Org Synth. 2021;18(5):483-492. https://doi.org/10.2174/1570179418666210203204930
37. Fadda AA, El-Latif EA, Bondock S, Samir A. Synthesis of some new pyrimidine and pyrimido[4,5-d]pyrimidine derivatives. Synth Commun. 2008 Nov 18;38(24):4352-4368. https://doi.org/10.1080/00397910802369216
38. Mohana KN, Kumar BNP, Mallesha L. Synthesis and biological activity of some pyrimidine derivatives. Drug Invention Today. 2013;5(3):216-222. https://doi.org/10.1016/j.dit.2013.06.009
39. Abo-Neima SE, El-Sheekh MM, Keshk RM. Synthesis and in vivo evaluation of pyrazolopyridine and pyridopyrazolopyrimidine derivatives as potent anticancer agents against Ehrlich Ascites carcinoma. Egypt J Chem. 2022;65(8):357-368. https://doi.org/10.21608/ejchem.2022.123456.5678
40. Mavrova AT, Wesselinova D, Tsenov YA, Denkova P. Synthesis, cytotoxicity and antimicrobial activity of some 4-substituted-2-phenylthieno[2,3-d]pyrimidines. Eur J Med Chem. 2009 Jan;44(1):63-9. https://doi.org/10.1016/j.ejmech.2008.03.002
41. Kerru N, Singh P, Koorbanally N, Raj R, Kumar V. Recent advances (2015-2016) in anticancer hybrids. Eur J Med Chem. 2017 Sep 8;142:179-212. https://doi.org/10.1016/j.ejmech.2017.07.033
42. Gao Y, Zhang Y, Wu H, Tian W, Chen X. Design, synthesis and biological evaluation of 4-anilinoquinazoline derivatives as potential EGFR inhibitors. Bioorg Med Chem Lett. 2018 Feb 1;28(3):163-167. https://doi.org/10.1016/j.bmcl.2017.12.044